HCC surgical specimens (data not shown) and the higher basal expression of GPC3 in $EpCAM^+$ cells than $EpCAM^-$ cells. Lentiviral knockdown of *GPC3* significantly reduced the sphere-forming ability of $EpCAM^+$ HCC cells. Additionally, replating assays and immunocytochemical analyses of EpCAM and AFP indicated that GPC3 regulated tumor-initiating HCC cells. Although it appears that DSF suppresses the tumorigenicity of tumor-initiating HCC cells in part by downregulating GPC3 expression, further analyses would be of importance to clarify the mechanisms underlying the downregulation of *GPC3* by DSF.

Finally, our findings successfully demonstrated that DSF significantly reduced the number of tumor-initiating HCC cells through apoptosis induction and the conversion to non-TICs. These effects appeared to be attributable to the activation of the ROS-p38 MAPK pathway and gene silencing with GPC3 (Figure 6G). Further analyses of the genes listed here are necessary to determine the effects of DSF. Recent reports showed that TICs of brain tumors reside in vascular niches in which endothelial cells maintain the TICs in an undifferentiated state [30]. Bevacizumab, a vascular endothelial growth factor (VEGF)-specific inhibitor, causes a drastic decrease in the number of TICs in vascular niches by inhibiting the self-renewal of TICs [31]. Although the niche for TICs in HCC remains to be elucidated, combination therapy using DSF and the anti-angiogenic multi-kinase inhibitor sorafenib might be effective in the eradication of tumor-initiating HCC cells.

Materials and Methods

Ethics statement

All experiments using the mice were performed in accordance with our institutional guidelines for the use of laboratory animals and approved by the review board for animal experiments of Chiba University (approval ID: 22–187).

Mice

Nonobese diabetic/severe combined immunodeficiency (NOD/SCID) mice (Sankyo-Lab Service, Tsukuba, Japan) were bred and maintained in accordance with our institutional guidelines for the use of laboratory animals.

Cell culture and reagents

The HCC cell lines were obtained from the Health Science Research Resources Bank (HSRRB, Osaka, Japan). DSF was kindly provided by Mitsubishi Tanabe Pharma Corporation. Cells were treated with DSF/$CuCl_2$ (0.1 or 1 μM) or 5-FU (1 μM; Sigma-Aldrich, St Louis, MO). Cells were treated with MG132 (10 μM, Cayman Chemical, Ann Arbor, MI), *N*-Acetyl-$_L$-cysteine (NAC) (10 μM, Sigma), and SB203860 (10 mM, Sigma).

Non-adherent sphere culture

For the sphere formation assay of Huh1, Huh6 and Huh7 cells, 1,000 cells were plated onto ultra-low attachment 6-well plates (Corning, Corning, NY). For the assay of PLC/PRF/5 cells, 500 cells were plated onto NanoCulture 24-well plates (Scivax, Kawasaki, Japan). The number of spheres (>100 μm in diameter) was counted on day 14 of culture. For the secondary sphere formation, a single cell suspension derived from primary colonies was obtained using a Neurocult chemical dissociation kit (StemCell Technologies, Vancouver, BC). Paraffin-embedded sections of the spheres were subjected to hematoxylin & eosin (H&E) staining and immunohistochemical staining with anti-EpCAM (Cell Signaling Technology, Beverly, MA) and anti-AFP (Dako Cytomation, Carpinteria, CA) antibodies.

Cell sorting and analysis

Single-cell suspensions were stained with allophycocyanin (APC)-conjugated anti-EpCAM antibody and anti-CD13 antibody (Biolegend, San Diego, CA) or APC-conjugated anti-CD133/1 antibody (Miltenyi Biotec, Auburn, CA). After the incubation, 1 μg/ml of propidium iodide was added to eliminate dead cells. Flow cytometirc cell sorting and analyses were performed using FACSAria or FACSCanto (BD Biosciences, San Jose, CA). Intracellular ROS levels were determined by flow cytometry using H2DCFDA (Sigma) and MitoSOX (Molecular Probes, Eugene, OR) staining.

Xenograft transplantation using NOD/SCID mice

A total of 2×10^6 Huh1 and Huh7 cells were suspended in DMEM and Matrigel (BD) (1:1). The cells were implanted into the subcutaneous space of the backs of NOD/SCID mice. DSF (10 or 50 mg/Kg) was administered intraperitoneally every other day.

Western blotting

DSF-treated HCC cells were subjected to Western blot analysis using anti-p38 (Santa Cruz Biotechnology, Santa Cruz, CA), anti-phospho-p38 (Cell Signaling Technology), and anti-tubulin (Oncogene Science, Cambridge, MA) antibodies. *ALDH2*-knockdown cells and *ALDH1*-and *ALDH2*-double knockdown cells were subjected to Western blotting using anti-ALDH1 (BD Biosciences) and anti-ALDH2 (Abcam, Cambridge, MA) antibodies. *GPC3*-knockdown cells selected by cell sorting for enhanced green fluorescent protein (EGFP) expression were also subjected to Western blot analysis using anti-GPC3 antibody (Santa Cruz Biotechnology).

Lentiviral production and transduction

A lentiviral vector carrying ERP (CS-H1-shRNA-RfA-ERP) expressing shRNAs against *ALDH2* (target sequence: sh-*ALDH2*-1, 5′-GCCCACTGTGTTTGGAGATGT-3′; sh-*ALDH2*-2, 5′-GCTGTCTTCACAAAGGATTTG-3′) was constructed for the double knockdown of *ALDH1* and *ALDH2*. Lentiviral vectors (CS-H1-shRNA-EF-1a-EGFP) expressing shRNAs against murine GPC3 (target sequence: sh-*GPC3*-1, 5′-GGCTCTGAATCTTG-GAATTGA-3′; sh-*GPC3*-2, 5′-GGGACTGATGATGGT-TAAACC-3′) were also constructed. Recombinant lentiviruses were produced as described elsewhere [32].

Generation of stable GPC3-expressing cells

Human GPC3 cDNA was cloned into a site upstream of IRES-neomycin in the pLP-IRESneo vector (Clontech, Palo. Alto, CA). Stable transfection into Huh1 cells with G418 selection was performed.

Reverse transcription-polymerase chain reaction (RT-PCR)

Quantitative RT-PCR was performed with an ABI PRISM 7300 Sequence Detection System (Applied Biosystems) using the Universal Probe Library System (Roche Diagnostics) according to the manufacturer's directions. The sequences of primers are listed in Table S3. Relative quantification was conducted by using the comparative cycle threshold (Ct) method.

Immunocytochemistry

After fixation with 2% paraformaldehyde and blocking in 10% goat serum, the cells were stained with anti-EpCAM (Cell Signaling Technology) and anti-phospho-p38 MAPK (Cell Signaling Technology) antibodies. Subsequently, the cells were incubated with Alexa-488–conjugated goat anti-mouse immuno-

globulin G (IgG) (Molecular Probes) and Alexa-555–conjugated goat anti-rabbit IgG (Molecular Probes). The cells were coverslipped using a mounting medium containing 4′, 6-diamidino-2-phenylindole dihydrochloride (DAPI) (Vector Laboratories, Burlingame, CA). For detection of apoptosis, the cells were also stained with an anti-active caspase-3 (CASP3) antibody (Chemicon, Temecula, CA), followed by incubation with Alexa-555 conjugated goat anti-rabbit IgG (Molecular Probes).

Microarray analysis

Cy3-labeled complementary RNA was hybridized to a SurePrint G3 Human GE 8×60 K microarray (Agilent Technologies, Santa Clara, CA). Array images were scanned using a DNA Microarray Scanner (Agilent) and analyzed using Feature Extraction version 10.27.1.1. (Agilent). Normalization was performed using GeneSpring GX11.5.1 (Agilent). The expression value (Signal) for each probe set was calculated using GeneSpring GX 12.0 (Agilent). Data were obtained for triplicate samples from three independent experiments. The data were subjected to normalization using GeneSpring normalization algorithms (Agilent). Only gene expression levels with statistical significance ($p< 0.05$) were recorded as being "detected" above background levels, and genes with expression levels below this statistical threshold were considered "absent." To identify differentially expressed genes in $EpCAM^+$ cells, we selected probe sets that exhibited gene expression changes with statistical significance as follows: (i) genes exhibiting a change greater than 1.5-fold ($p<0.05$), (ii) genes exhibiting a change from 1.0 to 1.5-fold ($p<0.01$), and (iii) switch-on type (upregulated from the "absent" to "present" level) and switch-off type genes (downregulated from the "present" to "absent" level) exhibiting a change greater than 4.0-fold ($p< 0.01$). Moreover, functional analyses were performed using Ingenuity Pathway Analysis (IPA) version 12402621 (Ingenuity Systems). To identify gene signatures after DSF or 5-FU treatment, gene set enrichment analysis (GSEA) was also conducted [33]. The raw data are available at http://www.ncbi.nlm.nih.gov/geo/(accession number; GSE 42318).

Statistical analysis

Data are presented as the mean ± SEM. Statistical differences between 2 groups were analyzed using the Mann-Whitney U test. P values less than 0.05 were considered significant.

Supporting Information

Figure S1 *In vitro* assays of HCC cells treated with DSF. (A) Dose-dependent and time-dependent inhibition of proliferation in HCC cells treated with DSF. *Statistically significant ($p<0.05$). (B) Detection of apoptotic cell death by immunostaining for active CASP3. Nuclear DAPI staining is shown in the insets. Scale bar = 100 μm. (C) Quantification of the percentage of apoptotic cells. *Statistically significant ($p<0.05$).
(TIF)

Figure S2 In vitro assay for *ALDH2*-knockdown and double knockdown of *ALDH1* and *ALDH2*. (A) Cells transduced with the indicated lentiviruses were subjected to Western blotting using anti-*ALDH2* and anti-tubulin (loading control) antibodies. (B) Cell proliferation in *ALDH2*-knockdown HCC cells was monitored by counting cell numbers. (C) Number of primary spheres generated from 1,000 cells at day 14 of culture. (D) Cells co-transduced with the indicated lentiviruses were subjected to Western blotting using anti-*ALDH1* antibody, anti-*ALDH2* and anti-tubulin (loading control) antibodies. (E) Bright-field (upper panels) images of non-adherent spheres at day 14 of culture. Scale bar = 100 μm. EGFP and RFP expression in double-knockdown spheres are shown in the insets. (F) Number of primary spheres generated from 1,000 cells at day 14 of culture.
(TIF)

Figure S3 Flow cytometric analyses of HCC cells treated with 5-FU. Flow cytometric profiles in cells treated with 5-FU (10μg/ml) for 48 hours. The percentages of positive fractions for the indicated markers are shown as the mean values for three independent analyses.
(TIF)

Figure S4 In vitro assay of sorted $EpCAM^-$ cells treated with DSF. (A) Non-adherent sphere formation assay on $EpCAM^-$ cells at day 14 of culture. Bright-field images are shown. Scale bar = 200 μm. (B) Number of large spheres generated from 1,000 HCC cells treated with DSF. *Statistically significant ($p< 0.05$). (C) Fluorescence images of $EpCAM^-$ HCC cells. The expression of p-p38 (red) was merged with nuclear DAPI staining (blue). Scale bar = 100 μm.
(TIF)

Figure S5 In vitro assay of sorted $EpCAM^+$ cells co-treated with DSF and a p38-specific inhibitor (SB203580). (A) Cell proliferation at 96 hours in culture. *Statistically significant ($p<0.05$). (B) Quantification of apoptotic cells based on the results of immunostaining for CASP3. *Statistically significant ($p<0.05$).
(TIF)

Figure S6 Gene expression profiles of $EpCAM^+$ cells treated with DSF or 5-FU. (A) Log2-fold heat map of genes involved in cell cycle in $EpCAM^+$ cells treated with DSF. (B) Quantitative RT-PCR analyses of cell cycle-related genes. *Statistically significant ($p<0.05$). (C) Gene set enrichment analysis (GSEA) of the proteasome pathway in $EpCAM^+$ cells treated with DSF or 5-FU. Both the normalized enrichment score (NES) and false discovery rate (FDR) are shown in each enrichment plot. (D) Log2-fold heat map of genes involved in the ROS scavenger pathway in $EpCAM^+$ cells treated with DSF or 5-FU.
(TIF)

Figure S7 Regulatory machinery of *GPC3* expression and loss-of-function assay of GPC3 in tumor-initiating HCC cells. (A) Quantitative RT-PCR analyses of *GPC3* expression in $EpCAM^+$ HCC cells co-treated with DSF and NAC or SB203580. *Statistically significant ($p<0.05$). (B) Quantitative RT-PCR analyses of *GPC3* expression in $EpCAM^+$ HCC cells treated with MG132. (C) Cell proliferation in *GPC3*-knockdown HCC cells at 96 hours in culture. *Statistically significant ($p<0.05$). (D) Quantification of apoptosis in cells transduced with indicated the lentiviruses based on the results of immunostaining for CASP3. *Statistically significant ($p<0.05$). (E) H&E staining and immunocytochemical analysis of EpCAM and AFP in spheres derived from $EpCAM^+$ cells. Scale bar = 20 μm. (F) Quantification of the percentage of $EpCAM^+$ or AFP^+ cells. *Statistically significant ($p< 0.05$).
(TIF)

Figure S8 Gain-of-function assay of GPC3 in Huh1 $EpCAM^+$ cells. (A) Cells transduced with the indicated retroviruses were subjected to Western blotting using anti-GPC3 and anti-tubulin (loading control) antibodies. (B) Proliferation of Huh1 $EpCAM^+$ cells at 96 hours in culture. The percentages of cells are shown. *Statistically significant ($p<0.05$). (C) Bright–field images of Huh1 $EpCAM^+$ cells in non-adherent sphere formation at day 14 of culture. Scale bar = 100 μm. (D) Number of large spheres derived from 1,000 $EpCAM^+$ cells on day 14 of culture. *Statistically

significant ($p<0.05$). (E) Number of secondary spheres 14 days after replating. *Statistically significant ($p<0.05$).
(TIF)

Table S1 Top five ontology terms with molecular and cellular function of upregulated genes after DSF or 5-FU treatment.
(DOC)

Table S2 Top five ontology terms with molecular and cellular function of downregulated genes after DSF or 5-FU treatment.
(DOC)

Table S3 Primer sequences used for real-time RT-PCR.
(DOC)

References

1. Jordan CT, Guzman ML, Noble M (2006) Cancer stem cells. N Engl J Med 355: 1253–1261.
2. Visvader JE, Lindeman GJ (2012) Cancer stem cells: current status and evolving complexities. Cell Stem Cell 10: 717–728.
3. Ji J, Wang XW (2012) Clinical implications of cancer stem cell biology in hepatocellular carcinoma. Semin Oncol 39: 461–472.
4. Rountree CB, Mishra L, Willenbring H (2012) Stem cells in liver disease and cancer: Recent advances on the path to new therapies. Hepatology 55: 298–306.
5. Chen D, Cui QC, Yang H, Dou QP (2006) Disulfiram, a clinically used anti-alcoholism drug and copper-binding agent, induces apoptotic cell death in breast cancer cultures and xenografts via inhibition of the proteasome activity. Cancer Res 66: 10425–10433.
6. Yip NC, Fombon IS, Liu P, Brown S, Kannappan V, et al. (2011) Disulfiram modulated ROS-MAPK and NFκB pathways and targeted breast cancer cells with cancer stem cell-like properties. Br J Cancer 104: 1564–1574.
7. Liu P, Brown S, Goktug T, Channathodiyil P, Kannappan V, et al. (2012) Cytotoxic effect of disulfiram/copper on human glioblastoma cell lines and ALDH-positive cancer-stem-like cells. Br J Cancer 107: 1488–1497.
8. Cen D, Gonzalez RI, Buckmeier JA, Kahlon RS, Tohidian NB, et al. (2002) Disulfiram induces apoptosis in human melanoma cells: a redox-related process. Mol Cancer Ther 1: 197–204.
9. Wang W, McLeod HL, Cassidy J (2003) Disulfiram-mediated inhibition of NF-kappaB activity enhances cytotoxicity of 5-fluorouracil in human colorectal cancer cell lines. Int J Cancer 104: 504–11.
10. Zhang H, Chen D, Ringler J, Chen W, Cui QC, et al. (2010) Disulfiram treatment facilitates phosphoinositide 3-kinase inhibition in human breast cancer cells in vitro and in vivo. Cancer Res 70: 3996–4004.
11. Moreb JS, Baker HV, Chang LJ, Amaya M, Lopez MC, et al. (2008) ALDH isozymes downregulation affects cell growth, cell motility and gene expression in lung cancer cells. Mol Cancer 7: 87.
12. Johansson B (1992) A review of the pharmacokinetics and pharmacodynamics of disulfiram and its metabolites. Acta Psychiatr Scand Suppl 369: 15–26.
13. Suzuki E, Chiba T, Zen Y, Miyagi S, Tada M, et al. (2012) Aldehyde dehydrogenase 1 is associated with recurrence-free survival but not stem cell-like properties in hepatocellular carcinoma. Hepatol Res 42: 1100–1111.
14. Ito K, Hirao A, Arai F, Matsuoka S, Takubo K, et al. (2004) Regulation of oxidative stress by ATM is required for self-renewal of hematopoietic stem cells. Nature 431: 997–1002.
15. Diehn M, Cho RW, Lobo NA, Kalisky T, Dorie MJ, et al. (2009) Association of reactive oxygen species levels and radioresistance in cancer stem cells. Nature 458: 780–783.
16. Yamashita T, Forgues M, Wang W, Kim JW, Ye Q, et al. (2008) EpCAM and alpha-fetoprotein expression defines novel prognostic subtypes of hepatocellular carcinoma. Cancer Res 2008;68:1451–1461.
17. Schaefer CF, Anthony K, Krupa S, Buchoff J, Day M, et al. (2009) PID: the Pathway Interaction Database. Nucleic Acids Res 37(Database issue): D674–679.
18. Science Signaling Web Site. Available: http://stke.sciencemag.org/cgi/cm/stkecm;CMP_10958 Accessed 2012 January 3.
19. Wong DJ, Nuyten DS, Regev A, Lin M, Adler AS, et al. (2008) Revealing targeted therapy for human cancer by gene module maps. Cancer Res 68: 369–378.
20. Midorikawa Y, Ishikawa S, Iwanari H, Imamura T, Sakamoto H, et al. (2003) Glypican-3, overexpressed in hepatocellular carcinoma, modulates FGF2 and BMP-7 signaling. Int J Cancer 103: 455–465.
21. Liu S, Li Y, Chen W, Zheng P, Liu T, et al. (2012) Silencing glypican-3 expression induces apoptosis in human hepatocellular carcinoma cells. Biochem Biophys Res Commun 419: 656–661.
22. Marchitti SA, Brocker C, Stagos D, Vasiliou V (2008) Non-P450 aldehyde oxidizing enzymes: the aldehyde dehydrogenase superfamily. Expert Opin Drug Metab Toxicol 4: 697–720.
23. Dollé L, Best J, Empsen C, Mei J, Van Rossen E, et al. (2012) Successful isolation of liver progenitor cells by aldehyde dehydrogenase activity in naïve mice. Hepatology 55: 540–552.
24. Ginestier C, Hur MH, Charafe-Jauffret E, Monville F, Dutcher J, et al. (2007) ALDH1 is a marker of normal and malignant human mammary stem cells and a predictor of poor clinical outcome. Cell Stem Cell 1: 555–567.
25. Tothova Z, Kollipara R, Huntly BJ, Lee BH, Castrillon DH, et al. (2007) FoxOs are critical mediators of hematopoietic stem cell resistance to physiologic oxidative stress. 128: 325–339.
26. Ito K, Hirao A, Arai F, Takubo K, Matsuoka S, et al. (2006) Reactive oxygen species act through p38 MAPK to limit the lifespan of hematopoietic stem cells. Nat Med 12: 446–451.
27. Ishimoto T, Nagano O, Yae T, Tamada M, Motohara T, et al. (2011) CD44 variant regulates redox status in cancer cells by stabilizing the xCT subunit of system xc- and thereby promotes tumor growth. Cancer Cell 19: 387–400.
28. Sawada Y, Yoshikawa T, Nobuoka D, Shirakawa H, Kuronuma T, et al. (2012) Phase I trial of a glypican-3-derived peptide vaccine for advanced hepatocellular carcinoma: immunologic evidence and potential for improving overall survival. Clin Cancer Res 18: 3686–3696.
29. Grozdanov PN, Yovchev MI, Dabeva MD (2006) The oncofetal protein glypican-3 is a novel marker of hepatic progenitor/oval cells. Lab Invest 86: 1272–1284.
30. Gilbertson RJ, Rich JN (2007) Making a tumour's bed: glioblastoma stem cells and the vascular niche. Nat Rev Cancer 7: 733–736.
31. Calabrese C, Poppleton H, Kocak M, Hogg TL, Fuller C, et al. (2007) A perivascular niche for brain tumor stem cells. Cancer Cell 11: 69–82.
32. Iwama A, Oguro H, Negishi M, Kato Y, Morita Y, et al. (2004) Enhanced self-renewal of hematopoietic stem cells mediated by the polycomb gene product Bmi-1. Immunity 21: 843–851.
33. Subramanian A, Tamayo P, Mootha VK, Mukherjee S, Ebert BL, et al. (2005) Gene set enrichment analysis: a knowledge-based approach for interpreting genome-wide expression profiles. Proc Natl Acad Sci U S A 102: 15545–15550.

Acknowledgments

The authors thank Dr. Fumihiko Kanai (Medical Corporation Eikenkai) and Dr. Motohisa Tada (Chiba University) for valuable discussions.

Author Contributions

Conceived and designed the experiments: TC ES KY YZ. Performed the experiments: TC ES KY YZ MO SM AS S. Koide. Analyzed the data: TC ES KY YZ TM SO YO AT. Contributed reagents/materials/analysis tools: TN TH TY S. Kaneko MM AI OY. Wrote the paper: TC AI.

PLOS ONE

Metformin, a Diabetes Drug, Eliminates Tumor-Initiating Hepatocellular Carcinoma Cells

Tomoko Saito[1,2☯], Tetsuhiro Chiba[1,2*☯], Kaori Yuki[1,2], Yoh Zen[3], Motohiko Oshima[2], Shuhei Koide[2], Tenyu Motoyama[1], Sadahisa Ogasawara[1], Eiichiro Suzuki[1], Yoshihiko Ooka[1], Akinobu Tawada[1], Motohisa Tada[1], Fumihiko Kanai[1], Yuichi Takiguchi[4], Atsushi Iwama[2], Osamu Yokosuka[1]

1 Department of Gastroenterology and Nephrology, Graduate School of Medicine, Chiba University, Chiba, Japan, **2** Department of Cellular and Molecular Medicine, Graduate School of Medicine, Chiba University, Chiba, Japan, **3** Institute of Liver Studies, King's College Hospital, London, United Kingdom, **4** Department of Medical Oncology, Graduate School of Medicine, Chiba University, Chiba, Japan

Abstract

Metformin has been widely used as an oral drug for diabetes mellitus for approximately 60 years. Interestingly, recent reports showed that metformin exhibited an anti-tumor action in a wide range of malignancies including hepatocellular carcinoma (HCC). In the present study, we investigated its impact on tumor-initiating HCC cells. Metformin suppressed cell growth and induced apoptosis in a dose-dependent manner. Flow cytometric analysis showed that metformin treatment markedly reduced the number of tumor-initiating epithelial cell adhesion molecule (EpCAM)$^+$ HCC cells. Non-adherent sphere formation assays of EpCAM$^+$ cells showed that metformin impaired not only their sphere-forming ability, but also their self-renewal capability. Consistent with this, immunostaining of spheres revealed that metformin significantly decreased the number of component cells positive for hepatic stem cell markers such as EpCAM and α-fetoprotein. In a xenograft transplantation model using non-obese diabetic/severe combined immunodeficient mice, metformin and/or sorafenib treatment suppressed the growth of tumors derived from transplanted HCC cells. Notably, the administration of metformin but not sorafenib decreased the number of EpCAM$^+$ cells and impaired their self-renewal capability. As reported, metformin activated AMP-activated protein kinase (AMPK) through phosphorylation; however its inhibitory effect on the mammalian target of rapamycin (mTOR) pathway did not necessarily correlate with its anti-tumor activity toward EpCAM$^+$ tumor-initiating HCC cells. These results indicate that metformin is a promising therapeutic agent for the elimination of tumor-initiating HCC cells and suggest as-yet-unknown functions other than its inhibitory effect on the AMPK/mTOR pathway.

Citation: Saito T, Chiba T, Yuki K, Zen Y, Oshima M, et al. (2013) Metformin, a Diabetes Drug, Eliminates Tumor-Initiating Hepatocellular Carcinoma Cells. PLoS ONE 8(7): e70010. doi:10.1371/journal.pone.0070010

Editor: Gianluigi Giannelli, University of Bari Medical School, Italy

Received April 8, 2013; **Accepted** June 13, 2013; **Published** July 29, 2013

Funding: This work was supported in part by grants for the Global COE program (Global Center for Education and Research in Immune System Regulation and Treatment) from the Ministry of Education, Culture, Sports, Science and Technology, Japan (http://www.jsps.go.jp/j-globalcoe/); grants from Core Research for Evolutional Science and Technology (CREST) of Japan Science and Technology Corporation (JST)(http://www.jst.go.jp/kisoken/crest/); and the Foundation for the Promotion of Cancer Research (http://www.fpcr.or.jp/). The funders had no role in study design, data collection and analysis, decision to publish, or preparation of the manuscript.

Competing Interests: The authors have declared that no competing interests exist.

* E-mail: techiba@faculty.chiba-u.jp

☯ These authors contributed equally to this work.

Introduction

Cancer stem cells (CSCs) or tumor-initiating cells (TICs) are a minor population of tumor cells with prominent tumorigenicity [1]. These cells are characterized by self-renewal capability and differentiation ability similar to those of normal stem/progenitor cells. Therefore, it has been believed that TICs play an important role in carcinogenesis, tumor growth, metastasis, and cancer recurrence. Recent progress in stem cell biology has enabled the identification and characterization of TICs in various cancers including hepatocellular carcinoma (HCC) [2]. Subsequently, the molecular machinery and signaling pathways involved in maintaining TICs have been vigorously explored [3]. Although the inhibitors of these molecules and signaling pathways are considered promising as TIC-targeting drugs, an effective therapy targeting TICs has yet to be developed.

Metformin is an oral drug that lowers blood glucose concentrations and has been widely used to treat type 2 diabetes mellitus [4]. The anti-diabetic action of metformin depends on the activation of AMP-activated protein kinase (AMPK), which contributes to a reduction in hepatic gluconeogenesis and an increase in glucose uptake in skeletal muscles [5]. Of interest, previous large case-control studies revealed that diabetic patients treated with metformin had a lower incidence of cancers than those treated with other diabetic drugs [6,7]. Various explanations for the efficacy of metformin have been proposed, such as the activation of AMPK, inhibition of insulin-like growth factor signaling, and the mTOR pathway [8]. Diabetes is known to be associated with an increase in the risk of developing HCC [9]. Indeed, the risk of HCC was significantly lower with metformin treatment than with sulphonylureas or insulin in chronic liver disease [10]. Furthermore, metformin reduced the risk of

recurrence of HCC after local ablation therapy [11]. Taken together, it is possible that metformin has direct effects on tumor-initiating HCC cells.

In the present study, we examined the effect of metformin on tumor-initiating HCC cells *in vitro*. We showed that metformin abolished their self-renewal capability and induced apoptosis in part through the activation of AMPK and subsequent inhibition of the mTOR pathway. Furthermore, xenograft transplantation experiments using nonobese diabetic/severe combined immunodeficient (NOD/SCID) mice demonstrated that metformin but not sorafenib decreased the number of TICs and impaired their self-renewal capability.

Results

Metformin Inhibited Cell Growth and Induced Apoptosis

To investigate the effect of metformin on HCC cells, we first examined cell growth and the frequency of apoptotic cells. Metformin treatment inhibited cell growth both time-dependently and dose-dependently in HCC cells and normal hepatocytes (Fig. 1A). Immunostaining of active caspase 3 (CASP3) showed that metformin induced apoptosis in a dose-dependent manner (Fig. 1B). The percentage of apoptotic cells in Huh1 cells, Huh7 cells, and normal hepatocytes treated with metformin (5 mM) was approximately five-fold, ten-fold, and seven-fold higher than that in control cells, respectively (Fig. 1C). Consistent with this result, flow cytometric analysis by staining with Annexin V and propidium iodide (PI) revealed that metformin caused apoptosis in a dose-dependent manner (Fig. 2).

Impact of Metformin Treatment on Tumor-initiating HCC Cells

The epithelial cell adhesion molecule $(EpCAM)^+$ fraction as well as the $CD133^+$ fraction was shown to include TICs in HCC [12,13]. We examined the expression of EpCAM and CD133 using flow cytometry to analyze the effect of metformin on tumor-initiating HCC cells. Metformin treatment (10 mM) decreased the $EpCAM^{high}$ fraction from 35.2% to 17.9% in Huh1 cells and from 33.0% to 12.2% in Huh7 cells (Fig. 3A). The $EpCAM^{high}$ fraction also decreased from 18.9% to 12.0% in normal hepatocytes after metformin exposure (Fig. 3A). Likewise, the $CD133^{high}$ fraction in Huh7 cells decreased from 40.5% to 26.1% (Fig. 3B), while the $CD133^+$ fraction was not detected in Huh1 cells or normal hepatocytes with or without metformin treatment. Taking into consideration the decrease in the total cell number, metformin appears to directly act on tumor-initiating HCC cells.

Sphere Assays of HCC Cells and Normal Hepatocytes Treated with Metformin

We then performed a non-adherent sphere formation assay of $EpCAM^+$ HCC cells and normal hepatocytes sorted by flow cytometry. EpCAM expression was markedly higher in the $EpCAM^+$ fraction than in the $EpCAM^-$ fraction by Western blot analysis (Fig. 4A). Unlike $EpCAM^+$ HCC cells, $EpCAM^+$ normal hepatocytes failed to form large spheres. Metformin treatment significantly impaired the formation of large spheres dose-dependently (Fig. 4B and 4C) and also the formation of secondary spheres after the replating of primary spheres (Fig. 4D). Together, these results indicate that metformin impaired the tumorigenicity of tumor-initiating HCC cells by inhibiting their self-renewal. To confirm the inhibitory effect of metformin on the self-renewal of tumor-initiating HCC cells, we conducted immunocytochemical analyses of the expression of EpCAM and α-fetoprotein (AFP), hepatic stem/progenitor cell markers, in the resultant spheres. A marked reduction in cells positive for EpCAM was observed in spheres generated from $EpCAM^+$ Huh1 cells (Fig. 5A). Because Huh1 cells only modestly produce AFP, no remarkable change in the number of cells positive for AFP was observed after metformin treatment. In contrast, metformin decreased both AFP^+ and $EpCAM^+$ cells in spheres generated from Huh7 cells treated with metformin (Fig. 5B). These results indicate that metformin impairs the self-renewal capability of TICs and accelerates their differentiation.

Impact of Metformin on Apoptosis, Cell Growth, and Cell Cycle

To examine the effect of metformin on cell proliferation, we conducted Western blotting of $EpCAM^+$ HCC cells and normal hepatocytes (Fig. 6A). As expected, cleaved poly (ADP-ribosyl) polymerase (PARP), a marker of apoptosis, was clearly detected in $EpCAM^+$ cells treated with metformin. The levels of proliferating cell nuclear antigen (PCNA) in $EpCAM^+$ cells treated with metformin decreased in a dose-dependent manner. The alteration in cyclin D1 and p21 expression levels caused by metformin differed between $EpCAM^+$ HCC cells and $EpCAM^+$ normal hepatocytes. Although metformin treatment increased the level of cyclin D1 in $EpCAM^+$ HCC cells, no marked changes in cyclin D1 expression were observed in $EpCAM^+$ normal hepatocytes. In addition, metformin treatment decreased the level of p21 in $EpCAM^+$ HCC cells, but conversely increased p21 expression level in $EpCAM^+$ normal hepatocytes.

AMPK/mTOR Pathway Following Metformin Exposure in $EpCAM^+$ HCC Cells and Normal Hepatocytes

Previous reports demonstrated that metformin suppressed mTOR signaling by activating AMPK in various cancer cells including HCC cells [14–16]. To examine whether this machinery also operated in $EpCAM^+$ HCC cells and normal hepatocytes, cells were subjected to Western blotting (Fig. 6B). In $EpCAM^+$ Huh7 cells and normal hepatocytes, the levels of phosphorylated AMPK increased after metformin exposure in a dose-dependent manner. Conversely, the levels of phosphorylated mTOR and phosphorylated S6 kinase decreased. However, $EpCAM^+$ Huh1 cells showed no change in the mTOR pathway, while the level of AMPK increased with exposure to metformin. These results raise the possibility that metformin impaired the self-renewal capability of tumor-initiating HCC cells in part by affecting the AMPK/mTOR pathway.

Anti-tumor Effects of Metformin and/or Sorafenib in Xenograft Transplantation Model

Sorafenib is an oral multikinase inhibitor with anti-angiogenic activity and has been approved for the treatment of advanced HCC [17]. To compare the anti-tumor effects of metformin and sorafenib, we conducted xenograft transplantation using NOD/SCID mice and administered metformin and/or sorafenib to recipient mice. Metformin and/or sorafenib were administered daily after the transplantation of 2×10^6 Huh7 cells into NOD/SCID mice. Both tumor initiation and growth were apparently suppressed by the metformin and sorafanib treatment (Fig. 7A and 7B). Tumor growth was further inhibited by the co-administration of metformin and sorafenib than by a single administration. Immunohistochemical staining of subcutaneous tumors for Ki-67 and CASP3 revealed that metformin and/or sorafanib treatment inhibited cell growth and induced apoptosis (Fig. 7C). Interestingly and importantly, the frequency of $EpCAM^+$ cells was markedly decreased in tumors treated with metformin, but not with

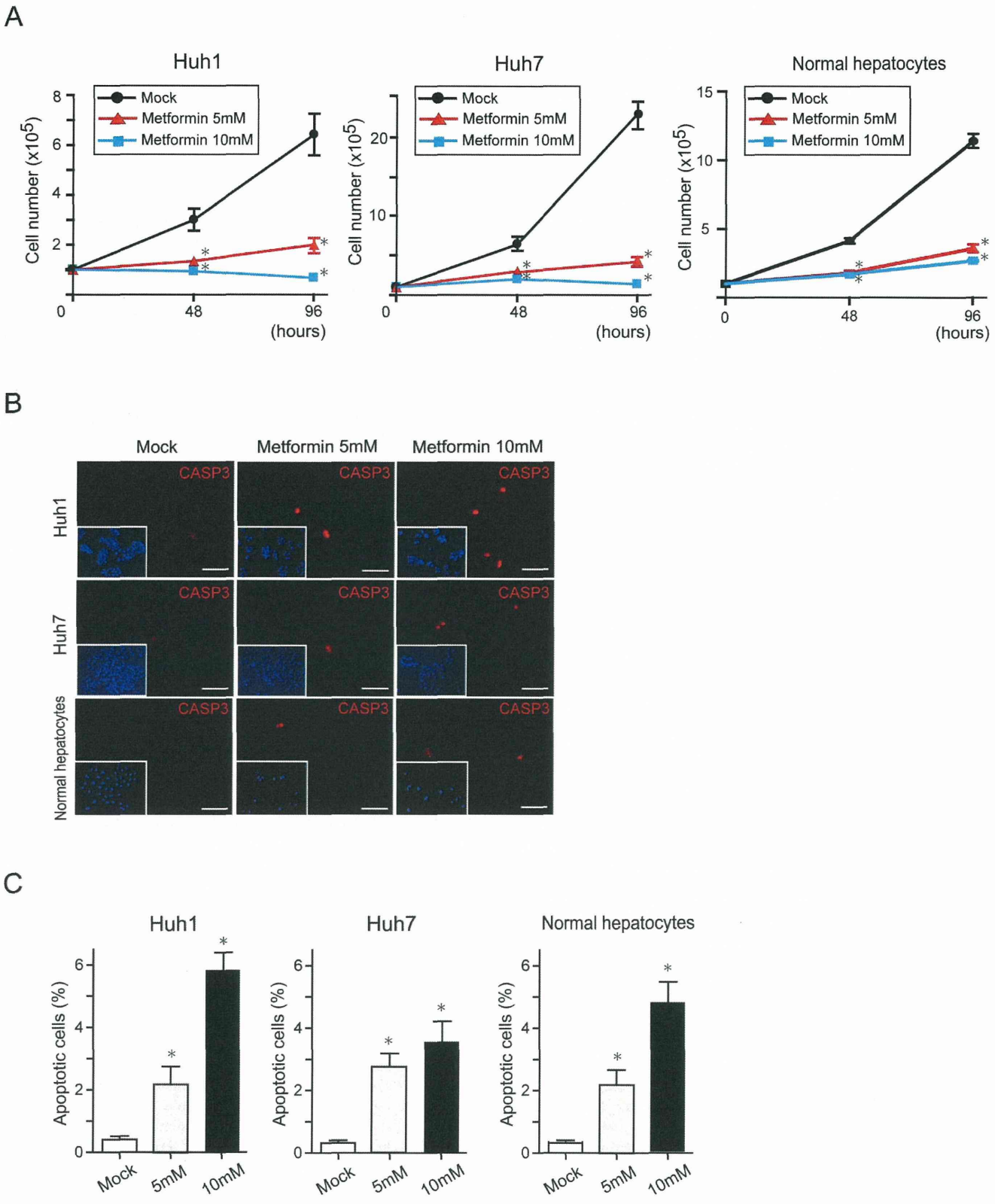

Figure 1. ***In vitro*** **assays of HCC cells and normal hepatocytes treated with metformin.** (A) Dose-dependent and time-dependent inhibition of the growth of HCC cells and normal hepatocytes treated with metformin. *Statistically significant ($p<0.05$). (B) Detection of apoptotic cells by immunostaining of CASP3. Nuclear DAPI staining is shown in the insets. Scale bar = 100 μm. (C) Quantification of the percentage of apoptotic cells. *Statistically significant ($p<0.05$).
doi:10.1371/journal.pone.0070010.g001

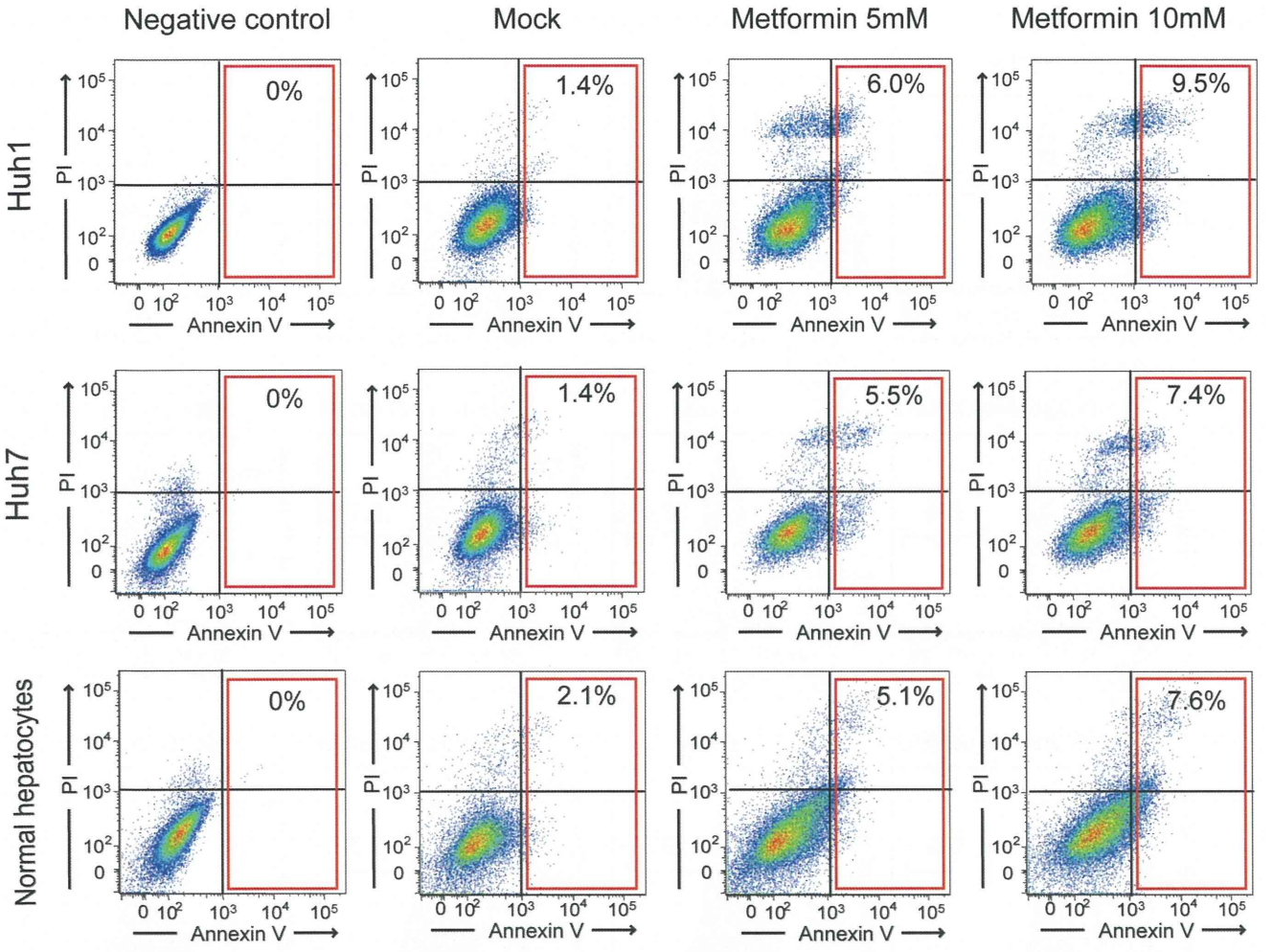

Figure 2. Detection of apoptotic cells by staining with Annexin V and PI using flow cytometry. The percentages of Annexin V-positive cells are shown as the mean values for three independent analyses.
doi:10.1371/journal.pone.0070010.g002

sorafenib (Fig. 7C). Co-treatment with metformin and sorafenib produced results similar to the single administration of metformin (Fig. 7C).

Re-analysis of Subcutaneous Tumors

Consistent with the pathological findings, flow cytometric analysis of xenograft tumors clearly demonstrated that metformin markedly reduced the number of tumor-initiating $EpCAM^+$ cells, whereas sorafenib did not (Fig. 8A). We conducted the non-adherent sphere formation assay of $EpCAM^+$ cells isolated from subcutaneous tumors. Metformin treatment as well as co-treatment with sorafenib markedly impaired primary sphere formation and even more severely impaired secondary sphere formation (Fig. 8B and 8C). In contrast, sorafenib treatment had very little effect on the formation of primary and secondary spheres (Fig. 8B and 8C). Taken together, metformin could be a therapeutic agent for the elimination of tumor-initiating HCC cells, at least in part by inhibiting their self-renewal capacity.

Discussion

A large number of studies have suggested that metformin has an anti-cancer effect in various types of malignancies including breast cancer and ovarian cancer, and even in HCC [14–16]. However, its efficacy against tumor-initiating HCC cells remains to be elucidated.

In this study, we first conducted cell growth assays in non-purified Huh1 and Huh7 cells treated with metformin. Consistent with previous reports, metformin treatment inhibited cell growth and induced apoptosis in both cell lines in dose-dependent and time-dependent manners. In addition, flow cytometric analysis showed a decrease in the proportion of $EpCAM^+$ and $CD133^+$ cells. These results prompted us to examine the direct action of metformin against tumor-initiating HCC cells. Sphere formation assays showed that metformin significantly suppressed the formation of spheres generated from $EpCAM^+$ TICs in a dose-dependent manner. Subsequent analysis for secondary sphere formation after replating showed similar results to those of primary sphere assays. In addition, immunocytochemical analysis revealed that metformin treatment reduced the number of $EpCAM^+$ and AFP^+ cells in primary spheres. Taken together, it appears that metformin impaired $EpCAM^+$ tumor-initiating HCC cells and simultaneously promoted the differentiation towards non-TICs.

Dependency on the mTOR pathway was shown to be higher in leukemic stem cells (LSCs) than in normal hematopoietic stem cells and the mTOR inhibitor rapamycin impaired the self-renewal of LSCs in leukemic mouse models [18]. mTOR signaling also makes a significant contribution to the maintenance of TICs in breast

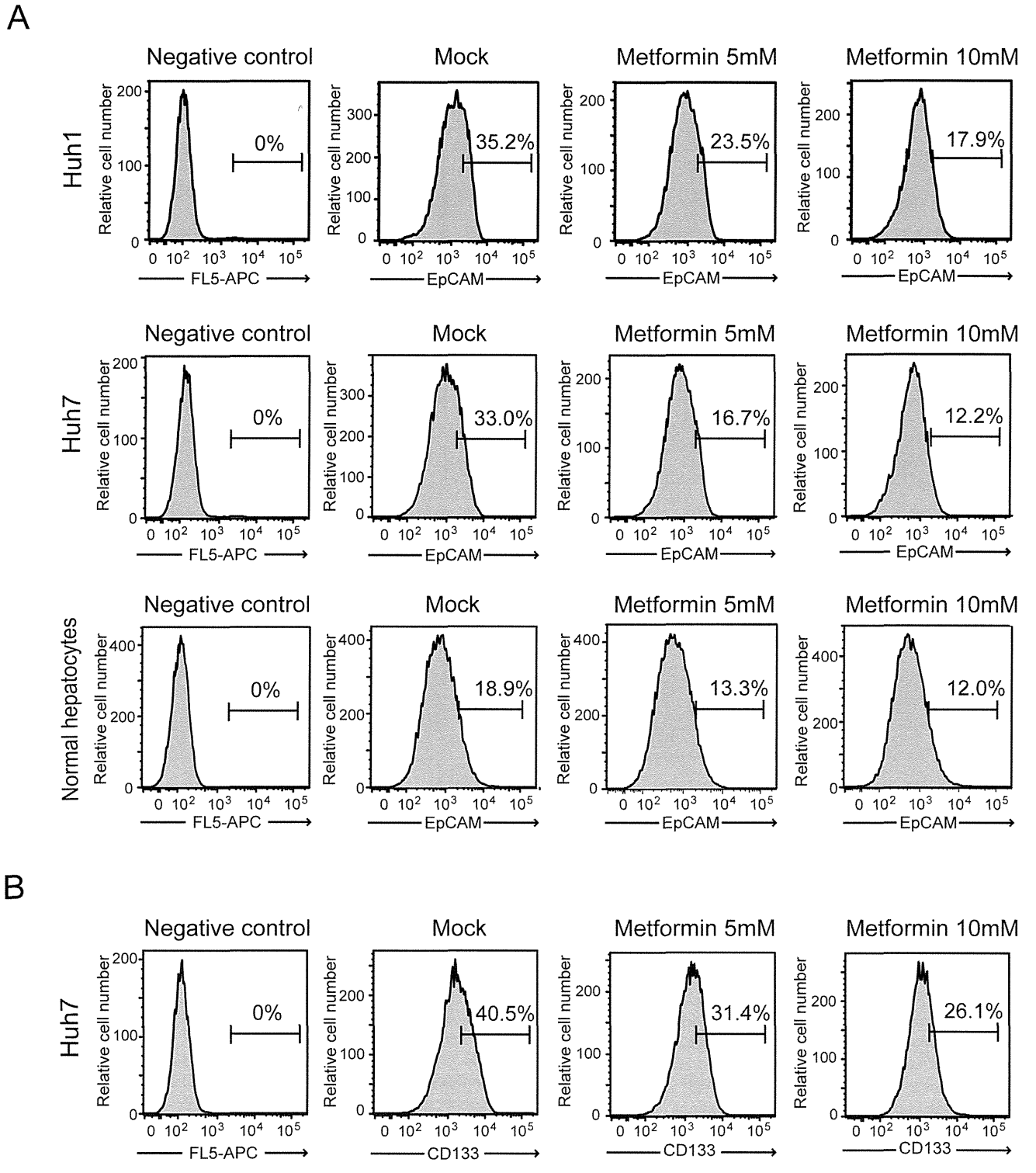

Figure 3. Flow cytometric profiles of HCC cells and normal hepatocytes treated with metformin (5 or 10 mM) for 72 hours. (A) The percentages of EpCAM$^+$ fractions are shown as the mean values for three independent analyses. (B) The percentages of CD133$^+$ fractions in Huh7 cells are shown as the mean values for three independent analyses.
doi:10.1371/journal.pone.0070010.g003

cancer and prostate cancer [19,20]. The aberrant activation of mTOR signaling was also observed in approximately 50% of patients with HCC [21,22]. The mTOR inhibitor, everolimus, which is currently undergoing clinical trials, exhibited an anti-tumor effect in some cases of advanced HCC [23]. Taken together, it appears that mTOR signaling plays an important role in hepatocarcinogenesis and the progression of HCC.

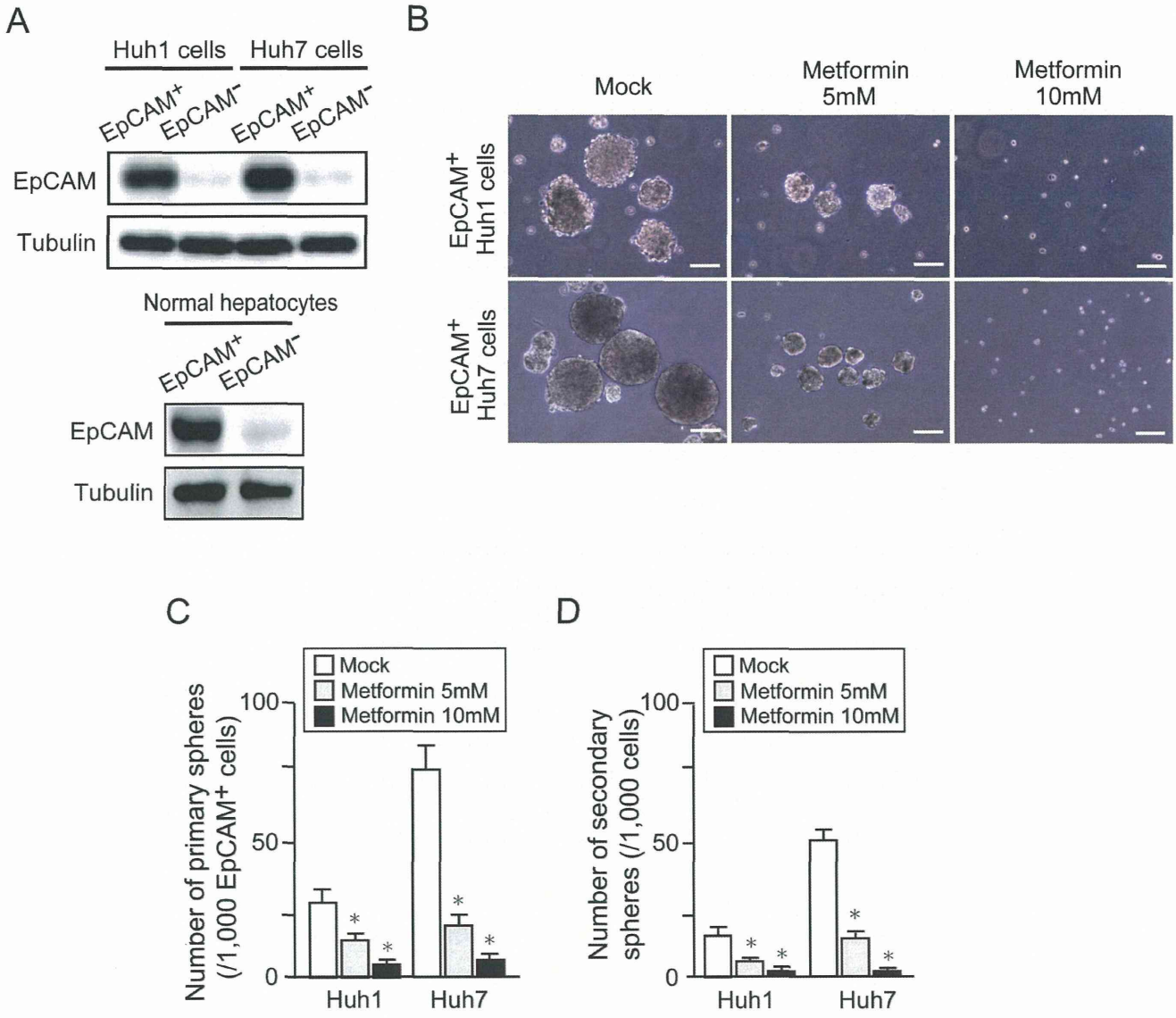

Figure 4. Non-adherent sphere formation assays of EpCAM$^+$ cells treated with metformin. (A) Western blot analysis of EpCAM expression in sorted EpCAM$^+$ cells. Tubulin was used as a loading control. (B) Bright-field images of the non-adherent spheres of EpCAM$^+$ HCC cells at day 14 of culture. Scale bar = 100 μm. (C) Number of large spheres generated from 1,000 EpCAM$^+$ cells treated with metformin. *Statistically significant ($p<0.05$). (D) Number of secondary spheres 14 days after replating. *Statistically significant ($p<0.05$).
doi:10.1371/journal.pone.0070010.g004

In the present study, metformin treatment apparently inhibited the mTOR pathway by phosphorylating AMPK in EpCAM$^+$ Huh7 cells. Considering that mTOR inhibitors suppressed the growth of Huh7 cells not only in culture but also in xenograft models [24,25], it is assumed that metformin exerted its anti-TIC effect by affecting the AMPK/mTOR pathway. In contrast, metformin did not alter the activity of the mTOR pathway in EpCAM$^+$ Huh1 cells despite inducing the phosphorylation of AMPK. One possible explanation for this is that mutations in the components of the mTOR pathway, which have been identified in many cancers and cancer cell lines, mask the effect of metformin in EpCAM$^+$ Huh1 cells [26]. Another possibility is that the mTOR pathway is not the major target of metformin and anti-tumor activity is exerted independent of the pathway. Several reports support this notion. For example, metformin was shown to cause cell cycle arrest by downregulating the expression of cyclin D1 and/or upregulating that of cyclin-dependent kinase inhibitors such as $p21^{Cip1}$ without inhibiting the mTOR pathway [27,28]. A previous report also attributed the anti-tumor activity of metformin to NF-kB inhibition in breast CSCs [29]. In addition, a recent study revealed a novel mechanism whereby metformin blocked glucagon-dependent glucose output from hepatocytes by reducing cyclic AMP and protein kinase A levels [30]. In the present study, metformin treatment suppressed the expression of cyclin D1 in EpCAM$^+$ HCC cells, but not in EpCAM$^+$ normal hepatcytes. Conversely, metformin increased p21 expression in EpCAM$^+$ normal hepatcytes, but not in EpCAM$^+$ HCC cells. Further analyses on the mechanisms of the anti-TIC activity of metformin are required.

Sorafenib is the sole molecular target drug clinically approved to treat advanced HCC. However, phase III trials have shown

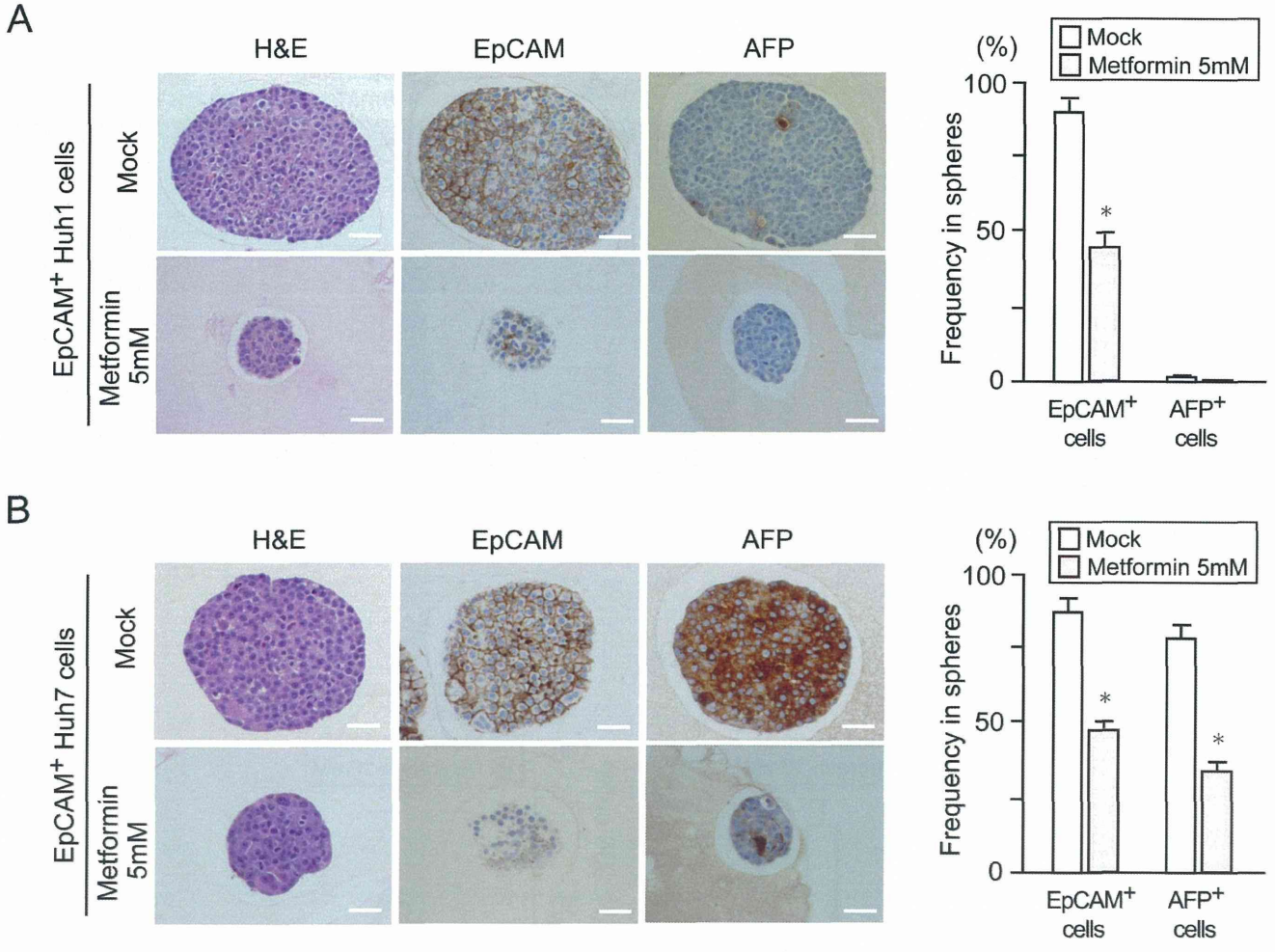

Figure 5. Immunostaining of EpCAM$^+$ cell-derived spheres. (A) Hematoxylin and eosin staining and immunocytochemical analysis of EpCAM and AFP in spheres derived from EpCAM$^+$ cells. Scale bar = 20 μm. (B) The percentage of EpCAM$^+$ cells or AFP$^+$ cells was determined. *, Statistically significant ($p<0.05$).
doi:10.1371/journal.pone.0070010.g005

that sorafenib prolonged median overall survival of patients with advanced HCC by no more than 3 months [31,32]. In our xenograft transplantation assay, treatment with metformin and sorafenib similarly suppressed the growth of subcutaneous tumors and co-treatment appeared to be more effective. Interestingly, both flow cytometric analysis and immunohistochemical analysis of xenograft tumors revealed that metformin significantly reduced the number of tumor-initiating EpCAM$^+$ cells, whereas sorafenib treatment had minimal effects on TICs. Taking these results into consideration, it is possible that the combined use of metformin and sorafenib exhibited stronger anti-tumor effect than sorafenib treatment alone in HCC.

In summary, metformin reduced the number and tumorigenicity of tumor-initiating HCC cells; however the involvement of the AMPK/mTOR pathway in its anti-tumor activity remains ambiguous. Because metformin suppressed cell growth and decreased the number of EpCAM$^+$ normal hepatocytes, further analysis might be necessary to determine whether metformin affects the function of normal hepatic stem/progenitor cells [33]. It is of importance to examine whether metformin might be of use for the elimination of TICs in HCC in clinical trials.

Materials and Methods

Ethics Statement

All experiments using mice were performed in accordance with our institutional guidelines for the use of laboratory animals and approved by the Review Board for Animal Experiments of Chiba University (approval ID: 22–187).

Mice and Reagents

NOD/SCID mice (Sankyo Laboratory Co. Ltd., Tsukuba, Japan) were bred and maintained in accordance with our institutional guidelines for the use of laboratory animals (approval ID: 22–187). Metformin (1,1-dimethylbiguanide hydrochloride) and sorafenib tosylate were purchased from Sigma-Aldrich (St. Louis, MO) and LKT laboratories (Saint Paul, MN), respectively.

Cell Culture and Sphere Formation Assay

The HCC cell lines, Huh1 and Huh7, were obtained from the Health Science Research Resources Bank (HSRRB, Osaka, Japan). Normal human hepatocytes were obtained from ACBRI (Kirkland, WA, USA). Cells were cultured in Dulbecco's modified Eagle's medium (Invitrogen Life Technologies, Carlsbad, CA) containing 10% fetal calf serum and 1% penicillin/streptomycin